Two-Dimensional Green's Function for an Elliptically Layered Cylindrical PEC Enclosure

Andrea Randazzo, Alessandro Fedeli, and Matteo Pastorino

***Abstract*—In this paper, a semi-analytical solution for the computation of the two-dimensional Green's function for a cylindrical PEC enclosure containing an arbitrary number of confocal elliptic dielectric layers is provided. The approach relies on an expansion of the Green's function into Mathieu functions, whose coefficients are found in an efficient way through a recursive procedure. The effectiveness of the technique is evaluated by comparisons with analytical formulas and against the results provided by independent numerical solvers. Moreover, the applicability to the solution of forward scattering problems using integral formulations is also assessed. In all the considered cases, the developed approach has been found to provide accurate results.**

***Index Terms*— Green's function, integral equations, electromagnetic scattering, stratified media.**

I. Introduction[1]

Green's functions are very important tools in theoretical and applied electromagnetics [1]–[3], since they represent the basic solutions of the wave equations when a unit point source (a line-current source in 2D settings or an elementary dipole in the 3D case) is considered, and, by exploiting the linearity of the problem, allow computing the field due to an arbitrary source distribution [4]. Due to their importance, several works dealt with the derivation of Green's functions in different configurations [5]–[8]. An important case is represented by cylindrical structures with canonical shape. Indeed, they often lead to analytical solutions [9], [10], which can be used as a reference for numerical techniques, and allows to simulate, in an approximate way, targets with elongated shapes. In particular, several works focused on layered circular cylinders, both considering the full 3D vector problem (leading to a dyadic Green's function) and the 2D case (resulting in a scalar Green's function) [11]–[15].

Another significant case is represented by layered media with elliptical cross section, since they allow representing non-fully symmetric objects and better approximating real targets. A first solution for computing the dyadic Green's function of a single-layer elliptical cylinder has been provided by Tai in [3], and further solving procedures has been later proposed [16], [17]. The scattering from elliptically layered structures has also been considered in several other works [18]–[22]. The multi-layer case has been addressed in a 2D transverse-magnetic (TM) configuration by the present Authors, considering media composed by all dielectric layers [23] and with a perfect electric conducting (PEC) core [24]. In particular, a semi-analytical solution based on the expansion of the Green's function in series of Mathieu functions [25], [26] has been devised. The coefficients are obtained through a recursive procedure relying on the application of the boundary conditions at the interfaces between layers. The developed solution can be used for computing the field produced by arbitrary z-directed sources. Moreover, it can be integrated into optimization schemes aimed at finding the optimal position of the source that satisfies some constraints on the radiated field (e.g., for maximizing the power), or used in inverse-source problems [27], [28].

Manuscript received May 13, 2021; revised December 14, 2021; accepted January 16, 2022. *(Corresponding author: Andrea Randazzo.)*

The authors are with the Department of Electrical, Electronic, Telecommunications Engineering and Naval Architecture (DITEN), University of Genoa, Genoa, Italy (e-mail: andrea.randazzo@unige.it, alessandro.fedeli@unige.it, matteo.pastorino@unige.it).

In this paper, enclosures bounded by a PEC elliptical surface, whose interior is composed by an arbitrary number of confocal elliptical dielectric layers, are considered. Such a configuration is of particular interest in different applicative scenarios. For example, in [29], [30] a homogeneous elliptical PEC enclosure is used to model the electromagnetic interaction of a point charge travelling inside an elliptical vacuum chamber (e.g., the CERN Proton Synchrotron). Moreover, the Green's functions of a PEC enclosure is fundamental in microwave imaging problems. Indeed, it represents the kernel of integral equations often used for modeling scattering problems in the presence of targets embedded in a dielectric medium, and thus may be used inside numerical procedures aimed at solving forward/inverse problems inside conducting chambers [31]–[34].

In particular, the solution originally presented in [23], [24] is extended for the first time to deal with the presence of an outer PEC boundary. This new configuration requires introducing significant modifications in the terms involved in the recursive procedure, in order to properly impose the boundary conditions between layers. Moreover, the possibility of using the developed Green's function for the solution of scattering problems involving dielectric targets inside a multilayer elliptical enclosure with PEC boundary is also addressed for the first time in this paper. The effectiveness of the developed solution is assessed by means of comparisons with the analytical solutions for homogeneous circular chambers and using a numerical solver based on the finite-difference time-domain (FDTD) method. Moreover, the capability of the approach in solving scattering problems is evaluated by exploiting an integral formulation using the Green's function as kernel, and the results are compared with the ones provided by the FDTD method.

The paper is organized as follows. The mathematical formulation of the procedure is detailed in Section II. Section III is devoted to the numerical validation of the approach. The application to scattering problems is discussed in Section IV. Conclusions follows.

II. Mathematical formulation

A cross section of the considered configuration is shown in Fig. 1. The medium is composed by L inner dielectric layers with complex dielectric permittivity ϵ_l, $l = 1, \dots, L$, whereas the outer layer is assumed to be a PEC material. The layers are separated by elliptical boundaries with semi-major axis a_l, $l = 1, \dots, L$, and half-focal distance d. All layers are confocal, i.e., they share the same foci.

The Green's function at a point (u, v) in the lth layer, when the source point is at the point (u', v') in the pth one, can be written as

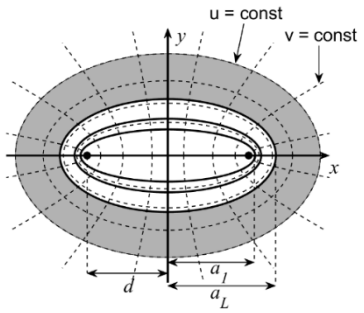

Fig. 1. Schematic representation of the considered configuration (cross section).

$g^{l,p}(u,v/u',v') = g^l_{ns}(u,v/u',v') + \delta_{l,p} g^p_s(u,v/u',v')$, where $\delta_{l,p}$ is the Kronecker's delta function. Elliptical coordinates (u,v), which are related to the rectangular coordinates through the relationships $x = d\cosh u \cos v$ and $y = d\sinh u \sin v$, are used [35]. The singular and non-singular terms g^p_s, g^l_{ns} are expressed as series of Mathieu functions [23] as

$$\begin{gathered} g^p_s(u,v/u',v') = \frac{j}{4}H^{(2)}_0\big(k_p R\big) = \\ \frac{j\pi}{2}\sum_{m=0}^{\infty}\frac{Mc^4_m(q_p,\breve{u})Mc^1_m(q_p,\hat{u})ce_m(q_p,v')ce_m(q_p,v)}{C^{pp}_{mm}} + \\ \frac{j\pi}{2}\sum_{m=1}^{\infty}\frac{Ms^4_m(q_p,\breve{u})Ms^1_m(q_p,\hat{u})se_m(q_p,v')se_m(q_p,v)}{S^{pp}_{mm}} \end{gathered} \tag{1}$$

$$\begin{gathered} g^l_{ns}(u,v/u',v') = \sum_{m=0}^{\infty}\big[e^l_{m,1}Mc^1_m(q_l,u) + \\ e^l_{m,2}Mc^2_m(q_l,u)\big]ce_m(q_l,v) + \sum_{m=1}^{\infty}\big[o^l_{m,1}Ms^1_m(q_l,u) + \\ o^l_{m,2}Ms^2_m(q_l,u)\big]se_m(q_l,v) \end{gathered} \tag{2}$$

where R is the distance between (u,v) and (u',v'), Mc^i_m and Ms^i_m are the even and odd radial Mathieu functions of kind i and order m, ce_m and se_m are the even and odd angular Mathieu functions of order m, $q_l = k_l^2 d^2/4$, $l = 1,\dots,L$, with $k_l^2 = \omega^2\epsilon_l\mu_0$ ($\mu_0 = 4\pi\times10^{-7}$ H/m being the magnetic permeability of vacuum), $\{C;S\}^{ij}_{mn} = \int_0^{2\pi}\{ce;se\}_m(q_i,v)\{ce;se\}_n(q_j,v)dv$, whereas $\breve{u} = u'$, $\hat{u} = u$ if $u \le u'$ and $\breve{u} = u$, $\hat{u} = u'$, otherwise.

Similarly to [23], [24], the expansion coefficients $e^l_{m,1}$, $e^l_{m,2}$, $o^l_{m,1}$, $o^l_{m,2}$ are found by imposing the boundary condition at the layers' interfaces through a Galerkin scheme using the angular Mathieu function $ce(q_{l+1},v)$ and $se(q_{l+1},v)$ as testing functions. In particular, by exploiting the orthogonality properties of the angular Mathieu functions, i.e., $\int_0^{2\pi} ce_m(q_i,v)se_n(q_j,v)dv = 0$, $\forall m,n,q_i,q_j$, and $\{C;S\}^{ii}_{mn} = 0$ when $m \ne n$, the following set of equations is obtained for $l = 1,\dots,L-1$

$$\begin{gathered} \sum_{m=0}^{\infty}C^{l(l+1)}_{mn}\Big[e^l_{m,1}Mc^1_m(q_l,u_l) + e^l_{m,2}Mc^2_m(q_l,u_l) + \\ \delta_{l,p}\frac{j\pi}{2}\frac{Mc^4_m(q_p,u_p)Mc^1_m(q_p,u')ce_m(q_p,v')}{C^{pp}_{mm}}\Big] = \\ C^{(l+1)(l+1)}_{nn}\Big[e^{l+1}_{n,1}Mc^1_n(q_{l+1},u_l) + e^{l+1}_{n,2}Mc^2_n(q_{l+1},u_l) + \\ \delta_{l+1,p}\frac{j\pi}{2}\frac{Mc^4_n(q_p,u')Mc^1_n(q_p,u_{p-1})ce_n(q_p,v')}{C^{pp}_{nn}}\Big], n = 0,1,\dots \end{gathered} \tag{3}$$

$$\begin{gathered} \sum_{m=1}^{\infty}S^{l(l+1)}_{mn}\Big[o^l_{m,1}Ms^1_m(q_l,u_l) + o^l_{m,2}Ms^2_m(q_l,u_l) + \\ \delta_{l,p}\frac{j\pi}{2}\frac{Ms^4_m(q_p,u_p)Ms^1_m(q_p,u')se_m(q_p,v')}{S^{pp}_{mm}}\Big] = \\ S^{(l+1)(l+1)}_{nn}\Big[o^{l+1}_{n,1}Ms^1_n(q_{l+1},u_l) + o^{l+1}_{n,2}Ms^2_n(q_{l+1},u_l) + \\ \delta_{l+1,p}\frac{j\pi}{2}\frac{Ms^4_n(q_p,u')Ms^1_n(q_p,u_{p-1})se_n(q_p,v')}{S^{pp}_{nn}}\Big],\ n = 1,2,\dots \end{gathered} \tag{4}$$

$$\begin{gathered} \sum_{m=0}^{\infty}C^{l(l+1)}_{mn}\Big[e^l_{m,1}DMc^1_m(q_l,u_l) + e^l_{m,2}DMc^2_m(q_l,u_l) + \\ \delta_{l,p}\frac{j\pi}{2}\frac{DMc^4_m(q_p,u_p)Mc^1_m(q_p,u')ce_m(q_p,v')}{C^{pp}_{mm}}\Big] = \\ C^{(l+1)(l+1)}_{nn}\Big[e^{l+1}_{n,1}DMc^1_n(q_{l+1},u_l) + e^{l+1}_{n,2}DMc^2_n(q_{l+1},u_l) + \\ \delta_{l+1,p}\frac{j\pi}{2}\frac{Mc^4_n(q_p,u')DMc^1_n(q_p,u_{p-1})ce_n(q_p,v')}{C^{pp}_{nn}}\Big],\ n = 0,1,\dots \end{gathered} \tag{5}$$

$$\begin{gathered} \sum_{m=1}^{\infty}S^{l(l+1)}_{mn}\Big[o^l_{m,1}DMs^1_m(q_l,u_l) + o^l_{m,2}DMs^2_m(q_l,u_l) + \\ \delta_{l,p}\frac{j\pi}{2}\frac{DMs^4_m(q_p,u_p)Ms^1_m(q_p,u')se_m(q_p,v')}{S^{pp}_{mm}}\Big] = \\ S^{(l+1)(l+1)}_{nn}\Big[o^{l+1}_{n,1}DMs^1_n(q_{l+1},u_l) + o^{l+1}_{n,2}DMs^2_n(q_{l+1},u_l) + \\ \delta_{l+1,p}\frac{j\pi}{2}\frac{Ms^4_n(q_p,u')DMs^1_n(q_p,u_{p-1})se_n(q_p,v')}{S^{pp}_{mm}}\Big], n = 1,2,\dots \end{gathered} \tag{6}$$

where DMc^i_m and DMs^i_m denote the derivatives of the even and odd radial Mathieu functions with respect to the radial elliptical coordinate u. In particular, (3)-(4) and (5)-(6) are obtained by imposing the continuity of the Green's function and of its derivative at the interfaces, respectively [23]. It is worth remarking that such conditions are obtained under the assumptions of confocal layers. Allowing the half-focal distance to be different for each layer would result in the need of using different sets of elliptic coordinates (which depends upon the half-focal distance) for describing the field. This is expected to introduce substantial changes in (3)-(6).

Moreover, by applying the boundary conditions to the outer PEC interface, i.e., for $l = L$, it results that

$$e^L_{n,2} = -\frac{Mc^1_n(q_L,u_L)}{Mc^2_n(q_L,u_L)}e^L_{n,1} - \delta_{L,p}\frac{j\pi}{2}\frac{Mc^4_n(q_L,u_L)Mc^1_n(q_L,u')ce_n(q_L,v')}{Mc^2_n(q_L,u_L)C^{LL}_{nn}} \tag{7}$$

$$o^L_{n,2} = -\frac{Ms^1_n(q_L,u_L)}{Ms^2_n(q_L,u_L)}o^L_{n,1} - \delta_{L,p}\frac{j\pi}{2}\frac{Ms^4_n(q_L,u_L)Ms^1_n(q_L,u')se_n(q_L,v')}{Ms^2_n(q_L,u_L)S^{LL}_{nn}} \tag{8}$$

If the series are truncated at the $(M-1)$th term, the following matrix equation, that link the expansion coefficients of the $(l+1)$th layer with those of the lth one, is obtained

$$\mathbf{B}_{l+1}\mathbf{x}_{l+1} = \mathbf{A}_l\mathbf{x}_l + \delta_{l,p}\mathbf{d}^p_{ext} - \delta_{l+1,p}\mathbf{d}^p_{int}, l = 1,\dots,L-1 \tag{9}$$

where the arrays $\mathbf{x}_l$, $l = 1,\dots,L$, which contain the expansion coefficients, are defined as (considering that for the inner dielectric layer it results $e^1_{m,2} = o^1_{m,2} = 0$ [23])

$$\mathbf{x}_l = \begin{cases} \big[e^2_{0,1},\ o^2_{1,1},\ \cdots,\ e^2_{M-1,1}\big]^t & l = 1 \\ \big[e^l_{0,1},e^l_{0,2},o^l_{1,1},o^l_{1,2},e^l_{1,1},\dots,e^l_{M-1,2}\big]^t & l = 2,\dots,L-1 \\ \big[e^L_{0,1},\ o^L_{1,1},\ \cdots,\ e^L_{M-1,1}\big]^t & l = L \end{cases} \tag{10}$$

and the matrices $\mathbf{A}_i$ and $\mathbf{B}_{i+1}$ are similar to those derived in [23], [24], i.e.,

$$\mathbf{A}_l = \begin{bmatrix} \mathbf{Ac}^l_{00} & 0 & \mathbf{Ac}^l_{01} & 0 & & \mathbf{Ac}^l_{0(M-1)} \\ 0 & \mathbf{As}^l_{11} & 0 & \mathbf{As}^l_{12} & \cdots & 0 \\ \mathbf{Ac}^l_{10} & 0 & \mathbf{Ac}^l_{11} & 0 & & \mathbf{Ac}^l_{1(M-1)} \\ 0 & \mathbf{As}^l_{21} & 0 & \mathbf{As}^l_{22} & & 0 \\ & \vdots & & & \ddots & \vdots \\ \mathbf{Ac}^l_{(M-1)0} & 0 & \mathbf{Ac}^l_{(M-1)1} & 0 & \cdots & \mathbf{Ac}^l_{(M-1)(M-1)} \end{bmatrix} \tag{11}$$

$$\mathbf{B}_{l+1} = \begin{bmatrix} \mathbf{Be}^{l+1}_0 & & \cdots & & 0 \\ & \mathbf{Bo}^{l+1}_1 & & & \\ \vdots & & \mathbf{Be}^{l+1}_1 & & \vdots \\ & & & \ddots & \\ 0 & & \cdots & & \mathbf{Be}^{l+1}_{M-1} \end{bmatrix} \tag{12}$$

Specifically, the submatrices $\mathbf{Ac}^l_{nm}$ and $\mathbf{As}^l_{nm}$ are defined as in equations (16) and (17) of [23], whereas $\mathbf{Be}^{l+1}_n$ ($n = 0,1,\dots,M-1$) and $\mathbf{Bo}^{l+1}_n$ ($n = 1,\dots,M-1$) are given by

$$\begin{gathered} \mathbf{Be}^{l+1}_n = C^{(l+1)(l+1)}_{nn}\begin{bmatrix} Mc^1_n(q_{l+1},u_l) & Mc^2_n(q_{l+1},u_l) \\ DMc^1_n(q_{l+1},u_l) & DMc^2_n(q_{l+1},u_l) \end{bmatrix}, \\ l = 1,..,L-2 \\ \mathbf{Be}^L_n = C^{LL}_{nn}\begin{bmatrix} Mc^1_n(q_L,u_{L-1}) - \frac{Mc^1_n(q_L,u_L)}{Mc^2_n(q_L,u_L)}Mc^2_n(q_L,u_{L-1}) \\ DMc^1_n(q_L,u_{L-1}) - \frac{Mc^1_n(q_L,u_L)}{Mc^2_n(q_L,u_L)}DMc^2_n(q_L,u_{L-1}) \end{bmatrix} \end{gathered} \tag{13}$$

$$\begin{gathered} \mathbf{Bo}^{l+1}_n = S^{(l+1)(l+1)}_{nn}\begin{bmatrix} Ms^1_n(q_{l+1},u_l) & Ms^2_n(q_{l+1},u_l) \\ DMs^1_n(q_{l+1},u_i) & DMs^2_n(q_{l+1},u_l) \end{bmatrix}, \\ l = 1,..,L-2 \\ \mathbf{Bo}^L_n = S^{LL}_{nn}\begin{bmatrix} Ms^1_n(q_L,u_{L-1}) - \frac{Ms^1_n(q_L,u_L)}{Ms^2_n(q_L,u_L)}Ms^2_n(q_L,u_{L-1}) \\ DMs^1_n(q_L,u_{L-1}) - \frac{Ms^1_n(q_L,u_L)}{Ms^2_n(q_L,u_L)}DMs^2_n(q_L,u_{L-1}) \end{bmatrix} \end{gathered} \tag{14}$$

Moreover, the source term $\mathbf{d}_{ext}^{p}$ is still given by equation (21) of [23], whereas $\mathbf{d}_{int}^{p}$ is now defined as

$$\mathbf{d}_{int}^{p} = \frac{j\pi}{2}\begin{bmatrix} Mc_0^4(q_p,u')Mc_0^1(q_p,u_{p-1})ce_0(q_p,v') \\ Mc_0^4(q_p,u')DMc_0^1(q_p,u_{p-1})ce_0(q_p,v') \\ Ms_0^4(q_p,u')Ms_0^1(q_p,u_{p-1})se_0(q_p,v') \\ Ms_0^4(q_p,u')DMs_0^1(q_p,u_{p-1})se_0(q_p,v') \\ \vdots \end{bmatrix} - \delta_{L,p}\frac{j\pi}{2}\begin{bmatrix} \frac{Mc_0^4(q_p,u_p)Mc_0^1(q_p,u')ce_0(q_p,v')Mc_0^2(q_p,u_{p-1})}{Mc_0^2(q_p,u_p)} \\ \frac{Mc_0^4(q_p,u_p)Mc_0^1(q_p,u')ce_0(q_p,v')DMc_0^2(q_p,u_{p-1})}{Mc_0^2(q_p,u_p)} \\ \frac{Ms_0^4(q_p,u_p)Ms_0^1(q_p,u')se_0(q_p,v')Ms_0^2(q_p,u_{p-1})}{Ms_0^2(q_p,u_p)} \\ \frac{Ms_0^4(q_p,u_p)Ms_0^1(q_p,u')se_0(q_p,v')DMs_0^2(q_p,u_{p-1})}{Ms_0^2(q_p,u_p)} \\ \vdots \end{bmatrix} \quad (15)$$

By applying recursively (9), a relationship between the innermost and outermost dielectric layers is obtained. In particular, setting $l = 1$, $\mathbf{x}_2$ can be written in terms of $\mathbf{x}_1$. This expression is substituted in the subsequent condition for $l = 2$, obtaining a relationship between $\mathbf{x}_3$ and $\mathbf{x}_1$. This procedure is iterated until all the boundary conditions are processed, resulting in the following relationship

$$\begin{aligned} &\mathbf{B}_L\mathbf{x}_L - \mathbf{A}_{L-1}\mathbf{D}_{L-2}\mathbf{x}_1 = \left(\mathbf{A}_{L-1}\mathbf{H}_{L-2,p} + \delta_{L-1,p}\mathbf{I}\right)\mathbf{d}_{ext}^{p} \\ &-\left(\mathbf{A}_{L-1}\mathbf{H}_{L-2,p-1} + \delta_{L,p}\mathbf{I}\right)\mathbf{d}_{int}^{p} \end{aligned} \quad (16)$$

where

$$\mathbf{H}_{l,p} = \begin{cases} \mathbf{C}_l \cdots \mathbf{C}_{p+1}\mathbf{B}_{p+1}^{-1} & if\ l > p \\ \mathbf{B}_{p+1}^{-1} & if\ l = p \\ \mathbf{0} & otherwise \end{cases} \quad (17)$$

with $\mathbf{C}_l = \mathbf{B}_{l+1}^{-1}\mathbf{A}_l$ and $\mathbf{D}_l = \mathbf{C}_l\mathbf{C}_{l-1}\cdots\mathbf{C}_1$.

From (16), it is finally possible to obtain the expansion coefficients for the innermost and outermost layers as

$$\begin{bmatrix} \mathbf{x}_1 \\ \mathbf{x}_L \end{bmatrix} = \mathbf{W}\begin{bmatrix} \mathbf{d}_{ext}^{p} \\ \mathbf{d}_{int}^{p} \end{bmatrix} \quad (18)$$

where $\mathbf{W}$ is a matrix of dimension $(4M-2)\times(4M-2)$ given by

$$\begin{aligned} &\mathbf{W} = [-\mathbf{A}_{L-1}\mathbf{D}_{L-2} \quad \mathbf{B}_L]^{-1} \\ &\left[\mathbf{A}_{L-1}\mathbf{H}_{L-2,p} + \delta_{L-1,p}\mathbf{I} \quad -\left(\mathbf{A}_{L-1}\mathbf{H}_{L-2,p-1} + \delta_{L,p}\mathbf{I}\right)\right] \end{aligned} \quad (19)$$

The coefficients for the remaining layers are found by recursively applying (9). It is worth noting that if $L = 1$ the problem can be directly solved by considering the boundary conditions in (7)-(8). In particular, since in the inner layer $e_{m,2}^{1} = o_{m,2}^{1} = 0$, it results

$$e_{n,1}^{1} = -\frac{j\pi}{2}\frac{Mc_n^4(q_1,u_1)Mc_n^1(q_1,u')ce_n(q_1,v')}{Mc_n^1(q_1,u_1)C_{nn}^{11}} \quad (20)$$

$$o_{n,1}^{1} = -\frac{j\pi}{2}\frac{Ms_n^4(q_1,u_1)Ms_n^1(q_1,u')se_n(q_1,v')}{Ms_n^1(q_1,u_1)S_{nn}^{11}} \quad (21)$$

Once the Green's function has been computed, the electric and magnetic fields due to an arbitrary z-directed current density $\mathbf{J}(u,v) = J_z(u,v)\hat{\mathbf{z}}$, with $(u,v) \in S$, can be obtained as $\mathbf{E}(u,v) = j\omega\mu_0\int_S J_z(u',v')g(u,v,u',v')\hat{\mathbf{z}}dS'$ and $\mathbf{H}(u,v) = \left[d\sqrt{\cosh^2 u - \cos^2 v}\right]^{-1}\int_S J_z(u',v')\left(-\frac{\partial}{\partial v}g(u,v,u',v')\hat{\mathbf{u}} + \frac{\partial}{\partial u}g(u,v,u',v')\hat{\mathbf{v}}\right)dS'$ (the derivatives of the Green's function with respect to u and v can be computed by replacing the radial and angular Mathieu functions with their corresponding derivatives [4]).

III. Numerical Validation

The effectiveness of the proposed approach is evaluated by means of simulations and comparisons with other numerical solvers.

As a first validation test, the capabilities of approximating the solution g_{circ} for a homogeneous circular cavity [36] when $d \to 0$ has been assessed. The cavity is assumed to be composed by a two-layer medium (to avoid reducing the computation to (20)-(21)) with semi-major axes $a_1 = 0.4\lambda_0$ and $a_2 = 0.5\lambda_0$. The half-focal distance d has been varied in the range $[10^{-6}, 0.35]$. In order to compare the solution with the one of a homogeneous circular structure, the two layers are assumed to have the same dielectric permittivity, i.e., $\epsilon_1 = \epsilon_2 = (3 - j0.6)\epsilon_0$. The source point has been located on the x axis at $x' = 0.1\lambda_0$. The working frequency has been set equal to 300 MHz. The number of terms used in the series is fixed to $M = 20$.

Fig. 2 shows the amplitude of the computed Green's function along the x and y axes for some values of the half-focal distance. As can be seen, the solution computed using (1)-(2) approximates very closely the values predicted by the analytical formula for the circular case as $d \to 0$. The same behavior can also be observed in the phase of the Green's function (not reported for sake of brevity).

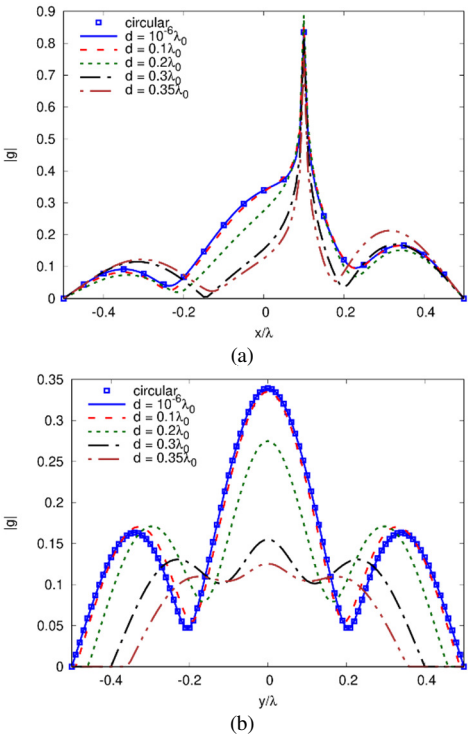

Fig. 2. Amplitude of the Green's function along the (a) x and (b) y axes for different values of the half-focal distance d. Homogeneous PEC enclosure.

In order to check the convergence properties of the developed solution, the error $e_{circ} = \|g - g_{circ}\|_2$ between the computed Green's function (in the case $d = 10^{-6}$) and the analytical solution for the circular cavity has been evaluated versus the number of terms M considered in the truncated series. The results are shown in Fig. 3 for different values of the number of layers, which are uniformly spaced in the chamber. In particular, it has been chosen to use layers with the same value of the permittivity in order to compare the results with the closed form solution for a homogeneous circular cavity, i.e., using a well-established reference case. However, the numerical procedure considers the presence of all the L layers, thus allowing to evaluate the numerical convergence considering all the terms of the series. Moreover, two different values of the dielectric permittivity of the chamber interior, i.e., $\epsilon = \{3\epsilon_0, 6\epsilon_0\}$, are considered to also assess the impact of this parameter.

In all the considered cases, a number of terms between approximately 10 and 18 is sufficient to achieve an error lower than 10^{-6}. The convergence rate estimated from the cases reported in the figure is exponential (the average R-squared coefficient obtained by fitting exponential curves is equal to 0.97). It is also worth remarking that in [24], when considering an elliptically layered structure with PEC core, it has been found that the number of required terms is comparable to $k_{max}a_{max}$, being k_{max} and a_{max} the maximum values of the wavenumber and semimajor axis among the layers, which is consistent with the results in Fig. 3. Consequently, in the following of the paper the number of terms has been set equal to 20, to guarantee that the series converge in the considered cases.

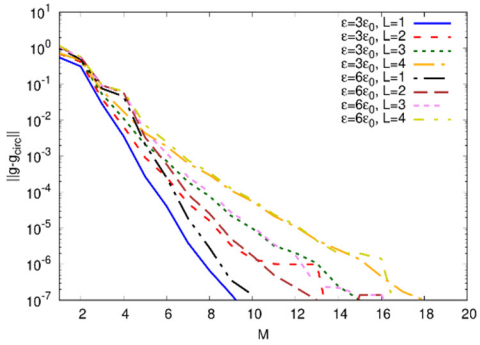

Fig. 3. Convergence behavior of the series. Homogeneous PEC enclosure.

As a second validation scenario, the results provided by the developed technique are compared with the ones obtained by a numerical solver based on the FDTD method (the gprMax open-source software [37] has been used). The considered chamber is composed by four layers with semi-major axes $a_1 = 0.15\lambda_0$, $a_2 = 0.25\lambda_0$, $a_3 = 0.35\lambda_0$, $a_4 = 0.5\lambda_0$, half-focal distance $d = 0.14\lambda_0$, and dielectric permittivities $\epsilon_1 = 2\epsilon_0$, $\epsilon_2 = (4 - j0.9)\epsilon_0$, $\epsilon_3 = (3 - j0.6)\epsilon_0$, $\epsilon_4 = (1.5 - j0.3)\epsilon_0$. It is worth remarking that lossy materials have been considered mainly for two reasons. First, this is a more general case, which requires the use of Mathieu functions with complex argument q. Second, the attenuation of the field inside the cavity allows to limit the duration of the time-domain simulations. Different positions of the source point along the x axis, i.e., $x' = \{0.1\lambda_0, 0.2\lambda_0, 0.3\lambda_0, 0.4\lambda_0\}$, have been considered, and the Green's function has been evaluated along the x and y axes. A square simulation domain with side $1.5\lambda_0$ enclosing the elliptical cylinder has been used and discretized into 640000 cells of side $1.875 \times 10^{-3}\lambda_0$. The temporal duration of the FDTD simulation has been set equal to $T = 0.5\ \mu s$. Such a value has been empirically chosen in order to guarantee that all transients are finished and the results are sufficiently stable. The frequency-domain data used for comparison are then extracted by applying a Fast Fourier Transform (FFT) to the computed time-domain data.

Fig. 4 report the amplitude of the Green's function along the x and y axes computed by using the developed approach, together with the values provided by the FDTD method. In all cases, there is a very good agreement between the two solutions, confirming the effectiveness of the developed approach. A similar behavior has also been observed in the phase (not reported for sake of brevity). Finally, to further analyze the convergence of the series, the quantity $\|g_{(M)} - g_{(20)}\|$, being $g_{(M)}$ the Green's function computed using M terms, is shown in Fig. 5 for different values of the half-focal distance (with $x' = 0.3\lambda_0$). As can be seen, the number of terms needed to converge is comparable to the one observed in Fig. 3, and this parameter is not significantly affected by the eccentricity.

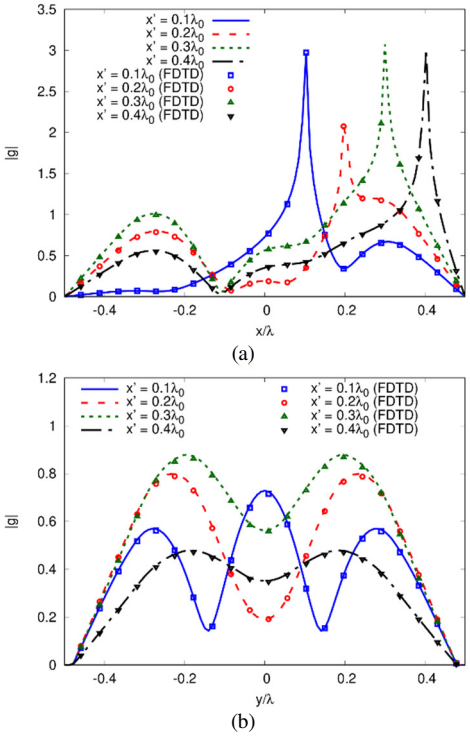

Fig. 4. Amplitude of the Green's function along the (a) x and (b) y axes for different values of the source position. Inhomogeneous four-layer chamber.

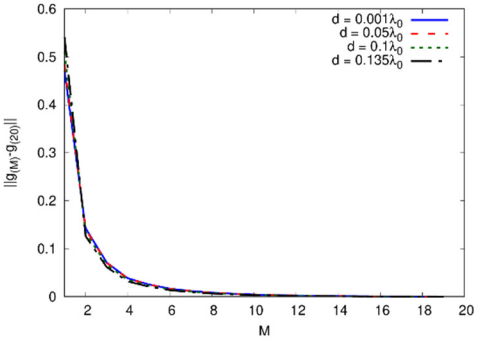

Fig. 5. Convergence behavior of the series. Inhomogeneous four-layer chamber.

IV. Scattering from Dielectric Objects Inside a Layered Elliptical Chamber

A relevant use of the developed Green's function is the computation of the field produced by objects embedded in an elliptical chamber, e.g., for use in imaging algorithms based on integral scattering formulations. The capabilities of the developed solving strategy to calculate the field in such conditions are evaluated and compared with those provided by a numerical solver based on the FDTD method (the gprMax software is again used, and the simulation parameters have been set as in the previous Section).

The considered configuration is shown in Fig. 6. A two-layer chamber is considered, with semi-major axes $a_1 = 0.35\lambda_0$ and $a_2 = 0.5\lambda_0$, half-focal distance $d = 0.2\lambda_0$, and dielectric permittivities $\epsilon_1 = (3 - j0.6)\epsilon_0$ and $\epsilon_2 = (2 - j1.2)\epsilon_0$. A line-current source with unit current amplitude located on the x axis at position $x' = 0.4\lambda_0$ is considered. The target is a void cylinder (i.e., with $\epsilon_{obj} = \epsilon_0$) with square cross section D_{obj} of side $l_{obj} = 0.2\lambda_0$ centered at position $(x_{obj}, y_{obj}) = (0.1\lambda_0, 0.1\lambda_0)$. When the target is not present inside the chamber, an incident electric field is produced, whose z-component is given by $e_{inc}(\mathbf{r}) = j\omega\mu_0 I g(\mathbf{r}, \mathbf{r}')$, where g is the two-

dimensional Green's function for the elliptical chamber. The z-component of the total electric field is given by

$$e_{tot}(\mathbf{r}) = e_{inc}(\mathbf{r}) - k_0^2 \int_{D_{obj}} \Delta\epsilon(\mathbf{r}') e_{tot}(\mathbf{r}') g(\mathbf{r},\mathbf{r}') d\mathbf{r}' \qquad (22)$$

where $\Delta\epsilon(\mathbf{r}) = \epsilon_{obj} - \epsilon_{ell}(\mathbf{r})$, $\epsilon_{ell}(\mathbf{r})$ being the dielectric permittivity of the elliptically-layered background. A method of moments (MoM) with pulse basis functions and Dirac's delta testing function is used to numerically solve (22). The region D_{obj} occupied by the object is discretized into N square subdomains D_n of side δ and center $\mathbf{r}_n$, in which the electric field and the dielectric properties are assumed constant. The number of subdomains has been chosen to provide a side δ much smaller than the wavelength, in order to guarantee a sufficient accuracy of the solution. Specifically, the values $N = 100$ and $\delta = 0.02\lambda_0$ have been used. The resulting discrete problem can be written as

$$\bar{e}_{tot} = \bar{e}_{inc} + [G]\mathrm{diag}(\Delta\bar{\epsilon})\bar{e}_{tot} \qquad (23)$$

where $\bar{e}_{inc}$ and $\bar{e}_{tot}$ are arrays of length N containing the values of the incident and total electric field in the subdomains used to discretize D_{obj}, whereas $\mathrm{diag}(\Delta\bar{\epsilon})$ is a $N \times N$ diagonal matrix containing the discretized values of $\Delta\epsilon(\mathbf{r})$. The elements $[G]_{i,j} = -k_0^2 \int_{D_j} g(\mathbf{r}_i,\mathbf{r}')d\mathbf{r}'$ of the matrix $[G]$ are computed as:

$$[G]_{i,j} = \begin{cases} -k_0^2 g(\mathbf{r}_i,\mathbf{r}_j)\delta^2 & \mathbf{r}_i \neq \mathbf{r}_j \\ -\frac{k_0^2}{k_l^2}\left(j\frac{\pi}{2}k_l\sqrt{\frac{\delta^2}{\pi}}H_1^{(2)}\left(k_l\sqrt{\frac{\delta^2}{\pi}}\right)+1\right) & \mathbf{r}_i = \mathbf{r}_j \end{cases} \qquad (24)$$

where k_l is the wavenumber in the layer containing the point $\mathbf{r}_j$. The Green's function integral in the singular case $\mathbf{r}_i = \mathbf{r}_j$ is approximated using the closed-form formula for the free-space Green's function in the corresponding layer [38]. Once $\bar{e}_{tot}$ is obtained, the field in a generic point can be computed using again (22). A direct solver based on the LU decomposition is used for solving (23). In order to evaluate the robustness of the approach, the condition number of the matrix $[I] - [G]\mathrm{diag}(\Delta\bar{\epsilon})$ defining the linear problem to be solved by the MoM has been evaluated, and in the considered case it resulted equal to 1.48. Such a low condition number confirms that it is possible to obtain an accurate computation of the total field.

The amplitude of the electric field along the x and y axes computed by using the developed Green's function is shown in Fig. 7, together with the corresponding FDTD values. The incident electric field is also shown. As highlighted by these results, there is a very good agreement between the values computed by the MoM, in which the layered structure is taken into account inside the Green's function and only the object cross section is considered in (23), and the ones obtained by using the FDTD method, which instead requires to discretize the whole domain. A similar behavior has also been observed in the phase (not reported for sake of brevity). The corresponding computational times are reported in Table I. It is worth remarking that in the case of the MoM, the overall computational time can be split into two parts. The incident field and matrix computations, which may be quite time consuming, can be performed offline, and reused for obtaining the total field using different dielectric configurations of the inclusion inside the chamber. This latter operation requires a very limited time, thus allowing a significant time saving. Conversely, the FDTD method always requires solving a full propagation problem considering the whole enclosure. Moreover, the calculation of the Mathieu functions is not straightforward and may affect the computational time. Although efficient numerical schemes have been developed [19], [25], [26], when the argument q is small (e.g., for small eccentricity) it is possible to approximate them with Taylor expansions [39]–[41], thus reducing the computational complexity.

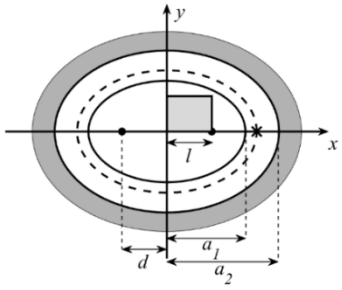

Fig. 6. Schematic representation of the considered configuration (cross section). Scattering from a target inside a layered elliptical chamber.

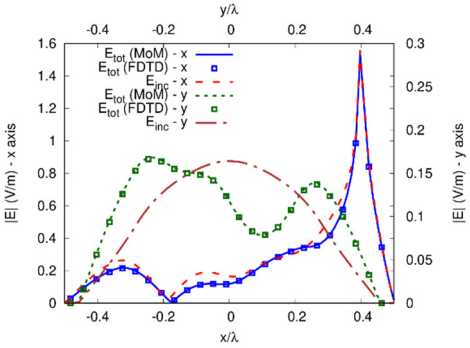

Fig. 7. Amplitude of the electric field along the x and y axes. Dielectric inclusion inside a two-layer elliptic chamber.

TABLE I
COMPUTATIONAL TIMES (PC EQUIPPED WITH AN INTEL(R) CORE(TM) I7-11700F @ 2.50GHZ CPU AND 16 GB OF RAM)

SOLVER	STEP	TIME [s]
MOM	Incident field computation (offline)	463
	Matrix fill time (offline)	983
	Total field computation (online)	0.021
FDTD	Total field computation (online)	393

V. CONCLUSION

A semi-analytical technique for computing the two-dimensional Green's function for a PEC enclosure containing multiple confocal dielectric layers has been presented. The approach is based on an expansion in series of Mathieu functions, whose coefficients are found through a recursive procedure involving the inversion of a single matrix. The effectiveness of the approach has been evaluated by comparing the computed values with analytical solutions and independent numerical solvers, showing that the developed solution is able to provide accurate results in all the considered cases. Moreover, the scattering from targets located inside the chamber has been addressed by means of an integral formulation using the Green's function as kernel for the integrals. Even in this case, the developed solution has been found to provide accurate results, which can be very helpful in the development of direct and inverse algorithms for imaging tasks. Future works will be aimed at the extension to the three-dimensional case, in order to obtain the full dyadic Green's function. Moreover, the case of cylinders with eccentric and/or not confocal layers will be addressed, too.

REFERENCES

[1] D. G. Dudley, *Mathematical Foundations for Electromagnetic Theory*. New York: IEEE Press, 1994.

[2] W. C. Chew, *Waves and Fields in Inhomogeneous Media*. Piscataway, NY: IEEE Press, 1995.

[3] C. Tai, *Dyadic Green Functions in Electromagnetic Theory*. Piscataway, NJ: IEEE Press, 1994.

[4] P. M. Morse and H. Feshbach, *Methods of Theoretical Physics*, vol. 2. New York, NY: McGraw-Hill, 1953.

[5] A. Alparslan, M. I. Aksun, and K. A. Michalski, 'Closed-form Green's functions in planar layered media for all ranges and materials', *IEEE Trans. Microw. Theory Techn.*, vol. 58, no. 3, pp. 602–613, Mar. 2010, doi: 10.1109/TMTT.2010.2040354.

[6] W. C. Chew, J. L. Xiong, and M. A. Saville, 'A matrix-friendly formulation of layered medium Green's function', *IEEE Antennas Wirel. Propag. Lett.*, vol. 5, pp. 490–494, 2006, doi: 10.1109/LAWP.2006.886306.

[7] S. Lambot, E. Slob, and H. Vereecken, 'Fast evaluation of zero-offset Green's function for layered media with application to ground-penetrating radar', *Geophys. Res. Lett.*, vol. 34, no. 21, 2007, doi: 10.1029/2007GL031459.

[8] B. Wu and L. Tsang, 'Fast computation of layered medium green's functions of multilayers and lossy media using fast all-modes method and numerical modified steepest descent path method', *IEEE Trans. Microw. Theory Techn.*, vol. 56, no. 6, pp. 1446–1454, Jun. 2008, doi: 10.1109/TMTT.2008.923901.

[9] J. J. Bowman, T. B. A. Senior, P. L. E. Uslenghi, and J. S. Asvestas, *Electromagnetic and Acoustic Scattering by Simple Shapes*. New York, NY: Hemisphere Pub. Corp., 1987.

[10] P. L. E. Uslenghi, 'Electromagnetic scattering by metallic cylinders perpendicularly truncated by a metal plane', *IEEE Trans. Antennas Propag.*, vol. 63, no. 5, pp. 2228–2236, May 2015, doi: 10.1109/TAP.2015.2408340.

[11] C. Tokgoz and G. Dural, 'Closed-form Green's functions for cylindrically stratified media', *IEEE Trans. Microw. Theory Techn.*, vol. 48, no. 1, pp. 40–49, Jan. 2000, doi: 10.1109/22.817470.

[12] S. Karan, V. B. Erturk, and A. Altintas, 'Closed-form Green's function representations in cylindrically stratified media for method of moments applications', *IEEE Trans. Antennas Propag.*, vol. 57, no. 4, pp. 1158–1168, Apr. 2009, doi: 10.1109/TAP.2009.2015796.

[13] Z. Guan, Y. Zhang, F. Han, C. Zhu, and Q. H. Liu, 'Fast exponentially convergent solution of electromagnetic scattering from multilayer concentric magnetodielectric cylinders by the spectral integral method', *IEEE Trans. Microw. Theory Techn.*, vol. 68, no. 6, pp. 2183–2193, Jun. 2020, doi: 10.1109/TMTT.2020.2973632.

[14] J. Wu, S. K. Khamas, and G. G. Cook, 'An efficient asymptotic extraction approach for the Green's functions of conformal antennas in multilayered cylindrical media', *IEEE Trans. Antennas Propag.*, vol. 58, no. 11, pp. 3737–3742, Nov. 2010, doi: 10.1109/TAP.2010.2077030.

[15] D. M. Pozar, 'A useful decomposition for the Green's functions of cylinders and spheres', *Radio Sci.*, vol. 17, no. 05, pp. 1192–1198, Sep. 1982, doi: 10.1029/RS017i005p01192.

[16] L.-W. Li, H.-G. Wee, and M.-S. Leong, 'Dyadic Green's functions inside/outside a dielectric elliptical cylinder: Theory and application', *IEEE Trans. Antennas Propag.*, vol. 51, no. 3, pp. 564–574, Mar. 2003, doi: 10.1109/TAP.2003.809854.

[17] L. W. Li, Z. C. Li, and M. S. Leong, 'Radiation due to an infinitely imposed current line source near a dielectric elliptic waveguide: A dyadic Green's function approach', *Radio Sci.*, vol. 39, no. 1, pp. 1–10, Feb. 2004, doi: 10.1029/2001RS002548.

[18] C. Yeh, 'The diffraction of waves by a penetrable ribbon', *J. Math. Phys.*, vol. 4, no. 1, pp. 65–71, Jan. 1963, doi: 10.1063/1.1703890.

[19] D. Erricolo, 'Acceleration of the convergence of series containing Mathieu functions using Shanks transformation', *IEEE Antennas Wirel. Propag. Lett.*, vol. 2, pp. 58–61, 2003, doi: 10.1109/LAWP.2003.813380.

[20] H. A. Ragheb and L. Shafai, 'Electromagnetic scattering from a dielectric-coated elliptic cylinder', *Can. J. Phys.*, vol. 66, no. 12, pp. 1115–1122, Dec. 1988, doi: 10.1139/p88-177.

[21] A. Sebak, L. Shafai, and H. A. Ragheb, 'Electromagnetic wave scattering by a two layered piecewise homogeneous confocal elliptic cylinder', *Radio Sci.*, vol. 26, no. 01, pp. 111–119, Jan. 1991, doi: 10.1029/90RS01843.

[22] O. Akgol, V. G. Daniele, D. Erricolo, and P. L. E. Uslenghi, 'Radiation from a line source shielded by a confocal elliptic layer of DNG metamaterial', *IEEE Antennas Wirel. Propag. Lett.*, vol. 10, pp. 943–946, 2011, doi: 10.1109/LAWP.2011.2167493.

[23] M. Pastorino, M. Raffetto, and A. Randazzo, 'Two-dimensional Green's function for scattering and radiation problems in elliptically-layered media', *IEEE Trans. Antennas Propag.*, vol. 62, no. 4, pp. 2071–2080, Apr. 2014, doi: 10.1109/TAP.2014.2299817.

[24] A. Fedeli, M. Pastorino, M. Raffetto, and A. Randazzo, '2-D Green's function for scattering and radiation problems in elliptically layered media with PEC cores', *IEEE Trans. Antennas Propag.*, vol. 65, no. 12, pp. 7110–7118, Dec. 2017, doi: 10.1109/TAP.2017.2761421.

[25] D. Erricolo, 'Algorithm 861: Fortran 90 subroutines for computing the expansion coefficients of Mathieu functions using Blanch's algorithm', *ACM Trans. Math. Softw.*, vol. 32, no. 4, pp. 622–634, Dec. 2006, doi: 10.1145/1186785.1186793.

[26] D. Erricolo and G. Carluccio, 'Algorithm 934: Fortran 90 Subroutines to Compute Mathieu Functions for Complex Values of the Parameter', *ACM Trans. Math. Softw.*, vol. 40, no. 1, p. 8:1-8:19, Oct. 2013.

[27] A. Abrashuly and C. Valagiannopoulos, 'Limits for absorption and scattering by core-shell nanowires in the visible spectrum', *Phys. Rev. Appl.*, vol. 11, no. 1, p. 014051, Jan. 2019, doi: 10.1103/PhysRevApplied.11.014051.

[28] Y. C. Hon, M. Li, and Y. A. Melnikov, 'Inverse source identification by Green's function', *Eng. Anal. Bound. Elem.*, vol. 34, no. 4, pp. 352–358, Apr. 2010, doi: 10.1016/j.enganabound.2009.09.009.

[29] S. Persichelli, N. Biancacci, M. Migliorati, L. Palumbo, and V. G. Vaccaro, 'Electromagnetic fields and Green's functions in elliptical vacuum chambers', *Phys. Rev. Accel. Beams*, vol. 20, no. 10, p. 101004, Oct. 2017, doi: 10.1103/PhysRevAccelBeams.20.101004.

[30] M. Migliorati, N. Biancacci, M. R. Masullo, L. Palumbo, and V. G. Vaccaro, 'Space charge impedance and electromagnetic fields in elliptical vacuum chambers', *Phys. Rev. Accel. Beams*, vol. 21, no. 12, p. 124201, Dec. 2018, doi: 10.1103/PhysRevAccelBeams.21.124201.

[31] A. Fedeli, V. Schenone, A. Randazzo, M. Pastorino, T. Henriksson, and S. Semenov, 'Nonlinear S-parameters inversion for stroke imaging', *IEEE Trans. Microw. Theory Techn.*, vol. 69, no. 3, pp. 1760–1771, Mar. 2021, doi: 10.1109/TMTT.2020.3040483.

[32] M. Asefi, A. Baran, and J. LoVetri, 'An experimental phantom study for air-based quasi-resonant microwave breast imaging', *IEEE Trans. Microw. Theory Techn.*, vol. 67, no. 9, pp. 3946–3954, Sep. 2019, doi: 10.1109/TMTT.2019.2906619.

[33] P. Mojabi and J. LoVetri, 'A novel microwave tomography system using a rotatable conductive enclosure', *IEEE Trans. Antennas Propag.*, vol. 59, no. 5, pp. 1597–1605, May 2011, doi: 10.1109/TAP.2011.2123066.

[34] J. Winges, L. Cerullo, T. Rylander, T. McKelvey, and M. Viberg, 'Compressed sensing for the detection and positioning of dielectric objects inside metal enclosures by means of microwave measurements', *IEEE Trans. Microw. Theory Techn.*, vol. 66, no. 1, pp. 462–476, Jan. 2018, doi: 10.1109/TMTT.2017.2708109.

[35] M. Abramowitz and I. A. Stegun, Eds., *Handbook of Mathematical Functions: With Formulas, Graphs, and Mathematical Tables*. New York, NY: Dover Publications, 1965.

[36] C. A. Balanis, *Advanced engineering electromagnetics*, 2nd ed. Hoboken, N.J: John Wiley & Sons, 2012.

[37] C. Warren, A. Giannopoulos, and I. Giannakis, 'gprMax: Open source software to simulate electromagnetic wave propagation for ground penetrating radar', *Comput. Phys. Commun.*, vol. 209, pp. 163–170, Dec. 2016, doi: 10.1016/j.cpc.2016.08.020.

[38] G. Gao, C. Torres-Verdin, and T. M. Habashy, 'Analytical techniques to evaluate the integrals of 3D and 2D spatial dyadic Green's functions', *Prog. Electromagn. Res.*, vol. 52, pp. 47–80, 2005, doi: 10.2528/PIER04070201.

[39] J. A. Roumeliotis and S. P. Savaidis, 'Cutoff frequencies of eccentric circular-elliptic metallic waveguides', *IEEE Trans. Microw. Theory Techn.*, vol. 42, no. 11, pp. 2128–2138, Nov. 1994, doi: 10.1109/22.330130.

[40] G. D. Tsogkas, J. A. Roumeliotis, and S. P. Savaidis, 'Electromagnetic scattering by an infinite elliptic dielectric cylinder with small eccentricity using perturbative analysis', *IEEE Trans. Antennas Propag.*, vol. 58, no. 1, pp. 107–121, Jan. 2010, doi: 10.1109/TAP.2009.2024527.

[41] C. A. Valagiannopoulos, 'Rigorous solution to plane wave scattering by an arbitrary-shaped particle embedded into a cylindrical cell of similar material', *Int. J. Antennas Propag.*, vol. 2009, p. e301461, Sep. 2009, doi: 10.1155/2009/301461.